Reentrant volume phase transition of hydrogel membrane of microcapsule

Takao Yamamoto[1], Toshiaki Dobashi[2*], Daisuke Suzuki[2] and Takayuki Narita[2]

[1] Department of Physics, and [2]Department of Biological and Chemical Engineering, Faculty of

Engineering, Gunma University, Kiryu, Gunma 376-8515, Japan

Running Head: Reentrant Volume Phase Transition

Telephone & Fax: (+81)(277)30-1477. E-mail: dobashi@bce.gunma-u.ac.jp

[1]Department of Biological and Chemical Engineering

[2] Department of Physics

* Corresponding author

Abstract

Reentrant volume phase transition of hydrogel wall membrane of microcapsules (MC) was first observed using MC suspensions consisting of poly(L-lysine-alt-terephthalic acid) wall and aqueous inner and outer solutions with different pHs. To analyze the dynamics of the reentrant phase transition, we extended the theory for the swelling and the shrinking dynamics of the microcapsule gel (Langmuir **2003**, 19, 4051-4054). In the theory, the microcapsule size and the force constant for the driving force which give rise to the size relaxation were chosen as the thermodynamic variables. The time course of the cross-sectional area of the microcapsules fitted well to the theoretical equations, and the time constants determined as the fitting parameters were discussed in terms of the force constant relaxation and the size relaxation.

I. Introduction

The reentrant phase transition has been observed in a variety of phase transitions such as ferromagnet-spin glass transition, insulator-metal phase transition, first-order phase transition of superconductivity, nematic-smectic phase transition, solvent-induced phase transition and multiphase phase transition of polymer solutions, and solid-liquid phase transition of ionic colloidal dispersions [1-10]. The mechanism of the reentrant phase transition has been discussed in terms of each characteristic interaction force.   Recently, multiple reentrant phase transitions were observed in both ionic and nonionic gels between the swollen and collapsed states. The unique behavior of the gel volume was attributed to a combination of hydrogen bonding and hydrophobic interactions between constituent polymer segments and analyzed by a mean field theory [11,12]. The dynamics of the reentrant transition, however, has not been studied yet.   When we use the conventional bulk gels, it is difficult to cover the whole time course and the pathway of the gel characteristic properties because it takes time consuming to reach the equilibrium state.   Thin hydrogel membranes of microcapsules has an advantage for the study of the dynamics because of their large surface area/volume ratio [13].   Furthermore, a unique phase transition dynamics of microcapsule gel membranes in both swelling and shrinking processes were explained by a single equation at different initial conditions [14].   The equation was derived by a theory assuming linear relationships for the rate of the change in the net charge and the cross sectional area against the differences from each

equilibrium value. Thus, it is very interesting to apply the theory to the reentrant volume phase transition consisting of both swelling and shrinking processes. In this study we measured the reentrant volume phase transition of Poly(L-lysine-alt-terephthalic acid) (PPL) wall membranes of microcapsules [13,15-17]. The PPL wall membrane has an isoelectric point at pH 2.3. The volume of the membrane takes the minimum around pH 4.5 (collapsed state), where a complex polyion structure is assumed to be formed [15]. There exist excess carboxylic groups above pH 4.5 and excess amino acid groups below pH 4.5 in the membrane. Swollen states appear at both high pH and very low pH. In a previous paper [14], we analyzed the dynamics between pH 4.5 and high pH, but the same picture should be applicable to the dynamics between very low pH and pH 4.5. This condition results in the reentrant phase transition by pH change between pHs above and below 4.5. The previous theory was extended to involve reentrant phase transition and utilized to analyze the experimental data.

II. Experimental results

   PPL microcapsules containing water were synthesized by an interfacial polycondensation reaction and dispersed in distilled water as described before [15]. An appropriate amount of buffer solution was added to it to obtain suspensions at a constant ionic strength of 0.1 and at desired pHs. As the salts in the buffer solution can easily pass through the membrane, the dispersing medium outside and

inside of the microcapsule membranes is assumed to be the same after rinsing the microcapsules with desired dispersing media for 24 h.

The distribution of the outer radius r_0 of the microcapsules were measured for microcapsules at pH=4.5 under an optical microscope. The resultant size distribution was fairly small; the percentage of microcapsules with each outer radius being 1.8% for 4.7-5.6μm, 4.7% for 5.6-6.9μm, 9.5% for 6.9-8.3μm, 15.5% for 8.3-10.1μm, 21.0% for 10.1-12.2μm, 20.3% for 12.2-14.7μm, 14.4% for 14.7-17.8μm, 7.6% for 17.8-21.6μm and 2.6% for 21.6-26.1μm. The ratio of the membrane thickness δ to r_0 was determined for selected microcapsules with different sizes at the same pH=3.8 by using a single particle light scattering method [13,18]. δ was linearly proportional to r_0, and the proportional coefficient was $(7.5 \pm 0.2) \times 10^{-3}$ in the range of r_0 being 9-14μm. It is reasonable to obtain the proportional relationship between δ and r_0 for the microencapsulation by means of the emulsion polymerization. This simple relationship ensures that an analysis of selected microcapsules represents typical characteristics of a collection of microcapsules at the same pH and pH change.

Microcapsules were incubated in a buffer solution at a predetermined pH = 4 (swollen state) for reaching the equilibrium state. Five μl of the microcapsule suspension at pH 4 was dripped on a cellulose mesh soaked in 10ml buffer solution at pH 7 (swollen state) in a petri dish settled on an optical microscope stage. The time course of the cross sectional area of microcapsules after a pH

jump was observed for microcapsules with different sizes under the microscope and recorded on a videotape.   The cross sectional area S of the microcapsules was measured on a monitor image reproduced from the videotape.   The suspension was also dripped in buffer solutions at pH 8 and 10, and the dynamics for microcapsules with similar sizes were traced.

Figure 1 shows the time courses of the cross-sectional area S by the pH quench from pH 4 to 7(a) (System A (smaller MC), B (larger MC)) and 8(b) (System C (smaller MC), D (larger MC)) for microcapsules with different sizes.   Quick decrease of S was followed by a long lag phase and S-shaped increase at all the conditions.   Both the time interval of the lag phase and the sharpness of the S-shaped increase of S are smaller for the smaller microcapsules.   Figure 2 shows the time course of S of microcapsules with a similar size for different pH quench depths (from pH=4 to 7(System B), 8(D), or 10(E)).   As the quench depth at the pH jump is increased, the time interval of the lag phase decreases and the sharpness of the S-shaped enhancement at the swelling becomes more noticeable.

III. Theoretical Approach

After we briefly summarize the theory for the shrinking and the swelling of the microcapsule gel discussed in the previous paper [14], then we extends it to deal with the reentrant behavior.

Brief survey of theory for time development for shrinking and swelling processes

The theory is based on the idea that the swelling and the shrinking are resulted from the competition between the elasticity and the charge repulsion of the membrane [14]. The elastic property is described in terms of the size; the cross sectional area is chosen as the variable expressing the size. The electric property is described by an introduction of "effective charge". Then, the thermodynamic state of a microcapsule is assumed to be expressed by the two parameters, the "effective" charge of the membrane q and the cross sectional area S of the microcapsule. Note that the cross sectional area is observed directly but the effective charge is not. Therefore, to compare the theoretical result with the experimental one, it is required that the final theoretical result is expressed in terms of only the cross sectional area.

On the basis of the conventional non-equilibrium thermodynamics, the relaxation process is expressed by the time development of the thermodynamic quantities q and S. Let us consider the time development from the initial state (q_I, S_I) to the final equilibrium state (q_{eq}, S_{eq}). The driving force may be proportional to the quench depth; the driving forces at the state (q, S) for the cross sectional area and for the effective charge are respectively given by

$$F_{el} = -K_{el}(S - S_{eq}),\qquad(1)$$

$$F_c = -K_c(q - q_{eq}),\qquad(2)$$

where K_{el} and K_c are positive force constants. The collapsed state is a quite special state. The presence of the lag time shows the high stability of this state. As discussed in the previous paper,

the swelling process from the collapsed state is quite slow.　This means that the repulsion force due to the membrane charge at the collapsed state is very small.　Since the magnitude of the charge repulsion is expressed by the magnitude of the effective charge, we can define the collapsed state by $q = 0$.　The high stability requires that the driving force for the size should disappear at the collapsed state.　In order that the driving force satisfies this requirement, the force constant K_{el} should be a function of q and vanish at $q = 0$.　The simplest expression of K_{el} is given by

$$K_{el} = K_0 q, \tag{3}$$

where K_0 is a positive constant.　For the effective charge, there are no special states at which the driving force vanishes.　Then, the force constant K_c can be expected to be independent of q and S.

　The time development equation expressing the relationship between the time t and the thermodynamic quantities $q(t)$ and $S(t)$ is given by the simultaneous equations in terms of the driving forces;

$$\frac{dS(t)}{dt} = \frac{1}{f} F_{el} = -Kq(t)(S(t) - S_{eq}), \tag{4}$$

$$\frac{dq(t)}{dt} = \Gamma_C F_C = -\alpha(q(t) - q_{eq}). \tag{5}$$

where f is the frictional coefficient and Γ_C is the kinetic coefficient for the effective charge. The constants K and α are given by $K = K_0 / f$ and $\alpha = \Gamma_C K_C$, respectively.　The solution of the simultaneous equations of (4) and (5) is given by

$$S(t) = S_{eq} + (S_I - S_{eq}) \exp\left[-Kq_{eq}t - \frac{K}{\alpha}(q_I - q_{eq})(1 - e^{-\alpha t})\right]$$
$$q(t) = q_I\, e^{-\alpha t} + q_{eq}(1 - e^{-\alpha t}) \tag{6}$$

Time development equation of reentrant behavior

The dynamics discussed in the above has been verified for the swelling and the shrinking

processes in the high pH region. From now on, we extend the above theory to deal with the

reentrant behavior. Let us regard the reentrant process as a combination of the shrinking process

from the swollen state at low pH to the collapsed state at pH 4.5 (Process I) and the swelling process

from the collapsed state to the swollen state at high pH (Process II). Although the signs of the

charge in the membrane for Process I and for Process II are different, the charge repulsion effect can

be described by the positive variable q. However, the value of α in Process I and in Process II

may be different, since the species of the ions relaxing the force constant is different; the values of

α for Process I and of Process II are respectively denoted by α_1 and α_2. This means that the

effective charge q is not a suitable variable to express the time development of the reentrant

process entirely. The force constant $K_{el} = K_{el}(t) = K_{el}(q(t))$ of the driving force for the size is a

more suitable variable since K_{el} is reasonably defined all over the pH region. In terms of K_{el},

eqs. (4) and (5) are rewritten as

$$\frac{dS(t)}{dt} = -\frac{1}{f} K_{el}(t)(S(t) - S_{eq}), \tag{7}$$

$$\frac{dK_{el}(t)}{dt} = -\alpha(K_{el}(t) - K_{el}^{eq}), \tag{8}$$

where K_{el}^{eq} is the force constant at the final equilibrium state.

9

The simultaneous equations of (7) and (8) can be understood as follows. The size of the microcapsules is relaxed by the driving force proportional to the deviation from the equilibrium value. The ion flow from the core to the outer dispersing medium changes the force constant K_{el}, and then the force constant depends on the time. The force constant relaxes and finally reaches the equilibrium value. The rate of the relaxation is proportional to the quench depth of the force constant. This picture based on the time dependent force constant is more natural than that based on the effective charge to discuss the entire reentrant process. Therefore, we adopt the force constant K_{el} as the thermodynamic variables to describe the reentrant dynamics instead of the effective charge q. In this picture, the collapsed state is characterized by the vanishing force constant; $K_{el} = 0$. The time course from the initial state (K_{el}^I, S_I) to the final equilibrium state (K_{el}^{eq}, S_{eq}) is given by

$$
\left.
\begin{aligned}
S(t) &= S_{eq} + (S_I - S_{eq}) \exp\left[-\frac{K_{el}^{eq}}{f} t - \frac{1}{\alpha f}(K_{el}^I - K_{el}^{eq})(1 - e^{-\alpha t}) \right] \\
K_{el}(t) &= K_{el}^I e^{-\alpha t} + K_{el}^{eq}(1 - e^{-\alpha t})
\end{aligned}
\right\}.
\tag{9}
$$

The initial state of the reentrant process at low pH, the collapsed state and the final state at high pH are, respectively, denoted by (K_{el}^L, S_L), $(0, S_0)$ and (K_{el}^H, S_H). Process I and Process II are regarded as the shrinking process from the state (K_{el}^L, S_L) to the state $(0, S_0)$ and the swelling process from $(0, S_0)$ to (K_{el}^H, S_H), respectively.

For Process I, $(K_{el}^I, S_I) = (K_{el}^L, S_L)$, $(K_{el}^{eq}, S_{eq}) = (0, S_0)$ and $\alpha = a_1$. Then, from eq.(9), we have the time course for the shrinking process;

$$\left. \begin{array}{l} S(t) = S_0 + (S_L - S_0)\exp\left[-\dfrac{K_{el}^L}{\alpha_1 f}(1 - e^{-\alpha_1 t})\right] \\[4mm] K_{el}(t) = K_{el}^L e^{-\alpha_1 t} \end{array} \right\} \qquad (10)$$

The function $S(t)$ shown above is convex downward. As discussed in the previous paper, the size S can not reach the collapsed size S_0 even in the limit $t \to \infty$ in the shrinking process, since the mechanisms inducing slower dynamics are neglected [14]. This merely shows that it takes quite a long time for the microcapsules to shrink completely. For Process II, $(K_{el}^I, S_I) = (0, S_0)$, $(K_{el}^{eq}, S_{eq}) = (K_{el}^H, S_H)$ and $\alpha = a_2$. Then, we have the time course for the swelling process;

$$\left. \begin{array}{l} S(t) = S_H + (S_0 - S_H)\exp\left[-\dfrac{K_{el}^H}{f}t + \dfrac{K_{el}^H}{\alpha_2 f}(1 - e^{-\alpha_2 t})\right] \\[4mm] K_{el}(t) = K_{el}^H (1 - e^{-\alpha_2 t}) \end{array} \right\}. \qquad (11)$$

The function $S(t)$ is an S-shaped increasing function. The properties of the functions (10) for Process I and (11) for Process II qualitatively agree with the experimental results shown in the previous section.

Eliminating the time t from eqs. (10) and (11), we have the pathway of the reentrant behavior on $K_{el} - S$ plane. The pathway is given for Process I by

$$S = S_0 + (S_L - S_0)\exp\left(\frac{K_{el} - K_{el}^L}{\alpha_1 f}\right), \qquad (12)$$

and for Process II by

11

$$S = S_H + (S_0 - S_H)\exp\left(\frac{K_{el} - K_{el}^H \ln\left(1 - K_{el}/K_{el}^H\right)}{\alpha_2 f}\right). \tag{13}$$

The curves expressing the shrinking process and the swelling process are different in the diagram,

since these processes are done in non-equilibrium.

IV. Analysis of Experimental Results

The experimental data for Process II (the swelling process) are quantitatively analyzed on the basis

of the theory, in contrast that Process I (the shrinking process) is hard to be analyzed on account of

rapid relaxation.   For convenience in the analysis of the swelling data, we introduce two time

constants $\tau_C = 1/\alpha_2$ and $\tau_M = f/K_{el}^H$, where τ_C and τ_M, respectively, correspond to the

relaxation times of the force constant (the effective charge) and the microcapsule size.   In terms of

the time constants, we rewrite eq. (11) as

$$S(t) = S_H + (S_0 - S_H)\exp\left[-\frac{t}{\tau_M} + \frac{\tau_C}{\tau_M}(1 - e^{-t/\tau_C})\right]. \tag{14}$$
$$K_{el}(t) = K_{el}^H (1 - e^{-t/\tau_C})$$

The inflection point of S-shaped increase of S(t) is given by

$$t = t_{IP} \equiv -\tau_c \ln\left[1 + \frac{1}{2}\frac{\tau_M}{\tau_c} - \frac{1}{2}\sqrt{\left(\frac{\tau_M}{\tau_c}\right)^2 + 4\left(\frac{\tau_M}{\tau_c}\right)}\right] \tag{15}$$

Near the inflection point, the function is approximately expressed by the linear equation;

$$S(t) \cong S(t_{IP}) + S'(t_{IP})(t - t_{IP}) \tag{16}$$

12

The slope of the line $S'(t_{IP})$ shows the sharpness of the S-shaped increase.

The parameters τ_M and τ_c were determined by a least squares fit. The data points and the calculated curves using the values of τ_c and τ_M are in fairly good agreement, as shown in Figs. 1 and 2. The sets of the resultant time constants (τ_C, τ_M) are (30.3s, 22.7s), (30.3s, 0.6s), (26.3s, 9.6s), (26.3s, 0.2s) and (17.0s, 0.1s), respectively, for the systems A, B, C, D, and E. From the comparison of the systems (A and B), and the systems (C and D), τ_M decreases with the size. This resulte in the decrease in the slope at the inflection point $S'(t_{IP})$, i.e., the sharpness of the S-shaped increase in the swelling process decreases. The decrease of τ_M with size could be attributed to the increase of the friction coefficient f with decreasing the membrane thickness δ r_o. With increasing the pH quench depth, τ_C and τ_M decrease simultaneously. This behavior of τ_M is also consistent with the theory which predicts a decrease of τ_M by decreasing the force constant K_{el}^H with the increase in pH quench depth.

In conclusion, a reentrant volume phase transition, swollen-collapsed-swollen phase transition, was first observed for microcapsules with hydrogel membrane. The phenomenological theory previously developed was extended to cover the reentrant phase transition by introducing a new aspect that force constant of the driving force for the size change was regarded as a dynamic constant. The entire volume behavior is explained using the theory qualitalively. The size and

quench depth dependence of the relaxation time τ_{M} in the swelling process observed and predicted

from the theory agree fairly well.

14

References

(1) Hamilton, A.R.; Simmons, M.Y.; Pepper, M.; Linfield, E.H.; Rose, R.D.; Richie, D.A. Phys. Rev. Lett. **1999**, 82, 1542.

(2) Yamanaka, J.; Yoshida, H.; Koga, T.; Ise, N.; Hashimoto, T. Phys. Rev. Lett. **1998**, 80, 5806.

(3) Matsubara, T.; Morishita, K.; Inawasiro, S. J. Phy. Soc. Jap. **1994**, 63, 416.

(4) Suzuki, T.; Sekiguchi, Y.; Tsuboi, T. J. Superconductivity **1999**, 12, 591.

(5) Davies, L. A.; Jackson, G.; Rull, L. F. Phys. Rev. Lett. **1999**, 82, 5285.

(6) Bassapa, G; Govind, A. S.; Madhusudana, N. V. J. Phys. (Paris) **1997**, 7, 1693.

(7) Matsuyama, A.; Tanaka, F. Phys. Rev. Lett. **1990**, 65, 341.

(8) Sales, M.; Yoshino, H. Phys. Rev. E **2002,** 65, 066131.

(9) Okayama, S.; Asaoka, H. Physica C **1999,** 633, 317.

(10) Suzuki, M.; Dobashi, T.; Mikawa, Y.; Yamamura, K.; Nakamura, M. J. Phy. Soc. Jap. **2000**, 69, 1741.

(11) Kawasaki, H.; Nakamura, T; Miyamoto, K.; Tokita, M. J. Chem. Phys. **1995**, 103, 6241.

(12) Annaka, M.; Tokita, M.; Tanaka, T.; Tanama, S.; Nakahira, T. J. Chem. Phys. **2000**, 112, 471.

(13) Dobashi, T.; Narita, T.; Masuda, J.; Makino, K.; Mogi, T.; Ohshima, H.; Takenaka, M.; Chu, B. Langmuir **1998**, 14, 745.

(14) Narita, T.; Yamamoto, T.; Suzuki, D.; Dobashi, T. Langmuir. **2003**, 19, 4051.

(15) Makino, K.; Miyauchi, E.; Togawa, Y.; Ohshima, H.; Kondo, T. In:Polymers of biological and biomedical significance, ACS Symposium Series 540, Chap.28, 1994, pp.314-323.

(16) Nagase, Y.; Kita, R.; Dobashi, T.; Kondo, T. Polym. Gels Networks. 1996, 4, 7.

(17) Miyauchi, E.; Togawa, Y.; Makino, K.; Ohshima, H.; Kondo, T. J. Microencapsulation **1992**, 9, 329.

(18) Dobashi, T.; Chu, B. In: Surface Characterization Methods, Surfactant Science Series 87, ed. by Milling, A.J., Chap.8, 1999, pp.249-268, Marcel Dekker, New York.

Figure captions

Figure 1. Time course of cross sectional area S of microcapsules with different sizes after a pH-jump from pH 4 to 7 (a) and to 8 (b). The symbols ( ), ( ), ( ), and ( ) denote the systems A, B, C, and D, respectively. Solid lines are calculated by using Eq. (14) with the parameters in the text. Dashed lines are drawn for the guide of eyes.

Figure 2. Time course of cross sectional area S of microcapsules with a similar size after a pH-jump from pH 4 to 7(Δ; system B), 8($\circ$; system D) and 10 ($\square$; system E). Solid lines are calculated by using Eq. (14) with the parameters in the text. Dashed lines are drawn for the guide of eyes.
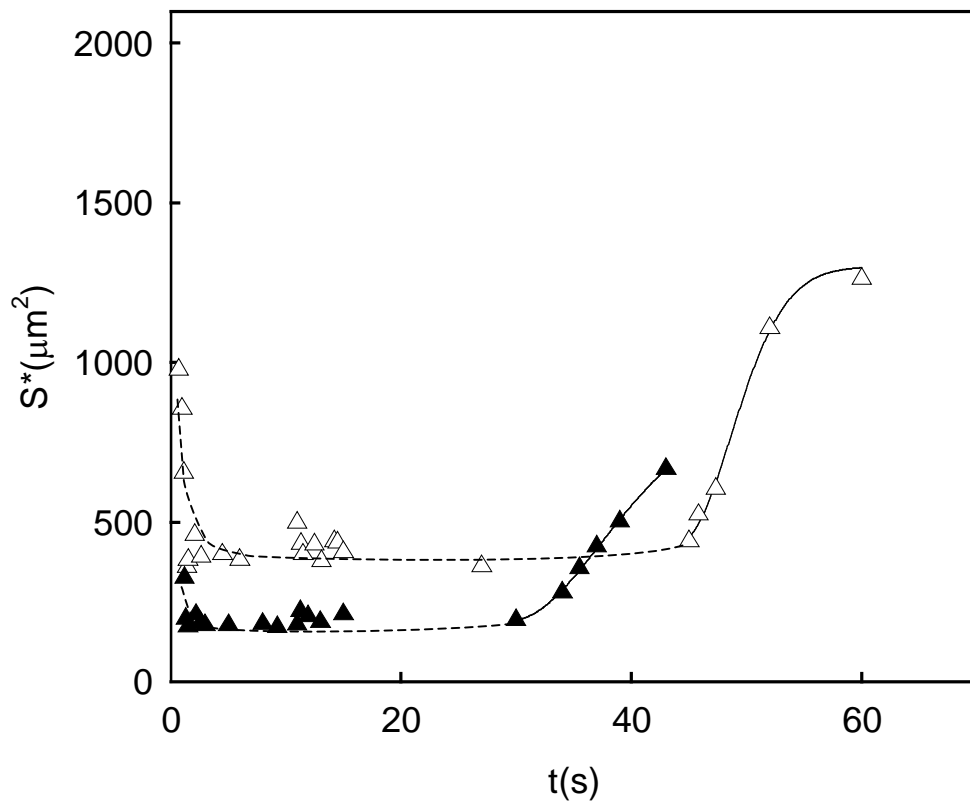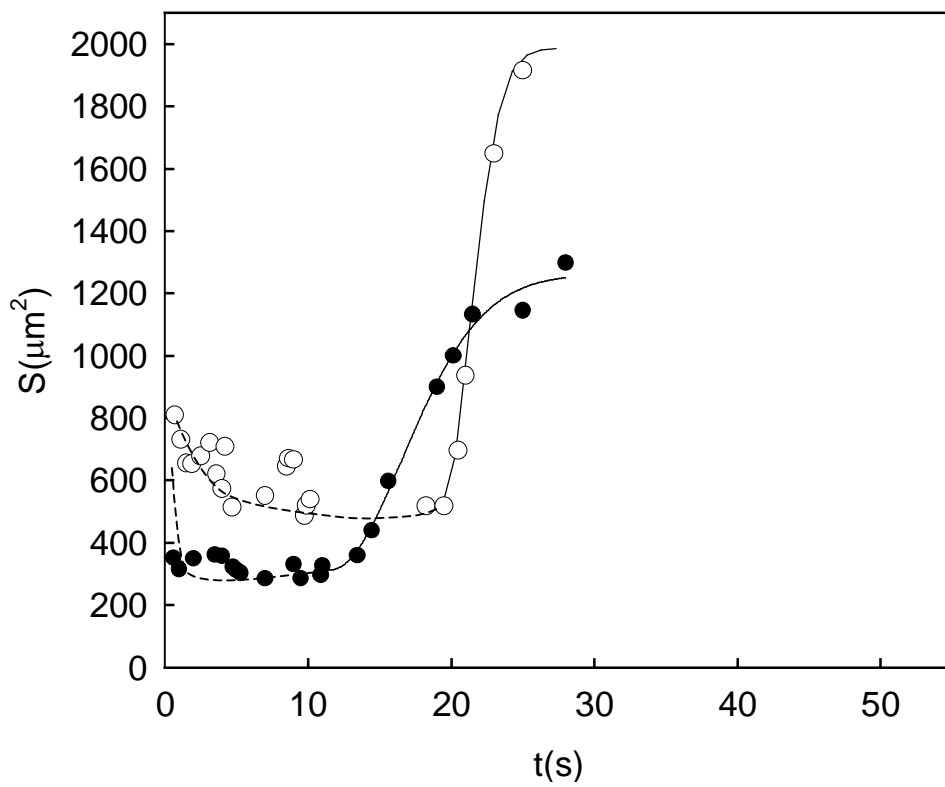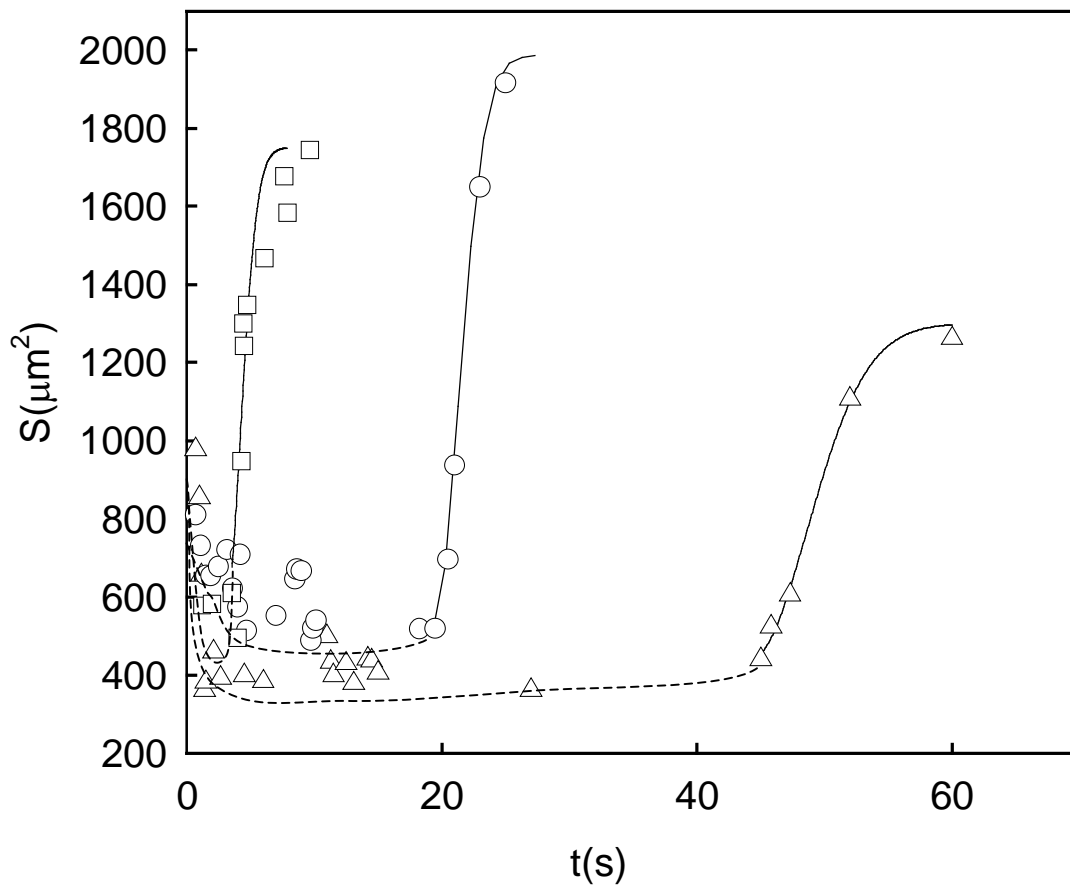
Figure 1 (a)

Figure 1 (b)

Figure 2